Generation of sub-17 fs vacuum ultraviolet pulses at 133 nm using cascaded four-wave mixing through filamentation in Ne

Takuya Horio,[1,2] Roman Spesyvtsev,[1,2] and Toshinori Suzuki[1,2,3,*]

[1]*Department of Chemistry, Graduate School of Science, Kyoto University, 606-8502 Kyoto, Japan*

[2]*Japan Science and Technology Agency, CREST, Sanbancho, Chiyoda-ku, Tokyo 102-0075, Japan*

[3]*RIKEN Center for Advanced Photonics, RIKEN, Wako, Saitama 351-0198, Japan*

**Corresponding author: suzuki@kuchem.kyoto-u.ac.jp*

Received June 27, 2014; revised September 18, 2014; accepted September 19, 2014; posted September 22, 2014 (Doc. ID 214744); published October 14, 2014

The sixth harmonic (6ω, 133 nm) of a Ti:sapphire laser is generated using cascaded four-wave mixing in filamentation propagation of the fundamental (ω) and the second harmonic (2ω) pulses through Ne gas. The method provides the 6ω pulse energy higher than 5 nJ/pulse at 1 kHz and a pulse duration shorter than 17 fs without dispersion compensation. © 2014 Optical Society of America

OCIS codes: (320.7090) Ultrafast lasers; (320.7150) Ultrafast spectroscopy; (140.7240) UV, EUV, and X-ray lasers.
http://dx.doi.org/10.1364/OL.39.006021

A vacuum UV (VUV) pulse in the 120–190 nm range can be generated using nonlinear optical crystals such as LiB_3O_5, $KB_5O_8 \cdot 4H_2O$, and SrB_4O_7 [1–3]; however, material dispersion limits the shortest pulse duration to ca. 100 fs. A shorter pulse duration can be obtained using rare gases as nonlinear media. For example, Kosma *et al.* [4] obtained a pulse duration of 11 fs at 162 nm by direct fifth harmonic (5ω) generation of a Ti:sapphire laser in Ar, although the conversion efficiency was quite low (6×10^{-6}).

Ultrashort pulses in the VUV region can be generated with much higher efficiencies using four-wave mixing (FWM) in filamentation propagation through rare gases. A long interaction length between laser pulses and a rare gas in filamentation provides a high conversion efficiency. Furthermore, the intensity clamping and the mode cleaning effects offer a high stability and a clean spatial mode, respectively [5]. Noack and coworkers employed collinear FWM of the fundamental (ω, 800 nm) and the third harmonic (3ω, 266 nm) of a Ti:sapphire laser in Ar to obtain a sub-50 fs sub-μJ 5ω pulse at 160 nm [6]; the conversion efficiency from 3ω to 5ω was 1.5×10^{-3}. The efficiency can be improved further by one-order of magnitude using noncollinear FWM, because the phase matching condition can be achieved by optimizing the crossing angle between the ω and 3ω pulses [7]. However, the phase matching angle depends on individual nonlinear processes, so that cascaded FWM has not been reported in the nonlinear geometry.

The cascaded FWM processes enable generation of multiple colors in the deep UV (DUV) and VUV regions, and it is highly useful for pump–probe spectroscopy. Zuo *et al.* [8] have demonstrated simultaneous generation of the fourth (4ω) and the fifth harmonics using the cascaded FWM processes of $3\omega + 3\omega - 2\omega \rightarrow 4\omega$ and $4\omega + 3\omega - 2\omega \rightarrow 5\omega$ in filamentation propagation through Ar. The pulse energies, 7.6 μJ at 198 nm and 0.6 μJ at 159 nm, were sufficiently high for pump–probe photoelectron spectroscopy. Horio *et al.* [9] generated 3ω, 4ω, and 5ω simultaneously by cascaded FWM processes in filamentation propagation of ω and 2ω through Ne. The maximum pulse energies were 10, 1, and 0.2 μJ for moderate input pulse energies of ω (0.43 mJ/pulse) and 2ω (0.37 mJ/pulse), and the cross-correlation time between the 4ω and 5ω pulses was 18 fs without dispersion compensation. In these studies, collinear geometries were employed.

These studies [8,9] indicate that the cascaded FWM in filamentation diminishes the pulse intensity by a factor of 10 for each increment of the harmonic order. Therefore, the cascaded FWM is expected to generate the sixth harmonic (6ω) with an intensity of ca. 10 nJ using our system. The 6ω pulse is highly useful for pump–probe photoelectron spectroscopy, because the 6ω photon energy exceeds the ionization energies of almost all aromatic molecules and enables direct one-photon ionization from the ground electronic state. Using 6ω as a probe pulse, pathways of photochemical reactions, including the ground state of a molecule and dissociated products, can be fully elucidated. On the other hand, commonly used UV light sources with lower photon energies do not enable single-photon ionization from the ground electronic state and low-lying excited states.

In this Letter, we report simultaneous generation of 6ω with 3ω, 4ω, and 5ω at 1 kHz. In order to generate and characterize the 6ω pulse, we have newly installed 6ω dichroic mirrors, a photodiode capable of measuring a VUV pulse energy at the level of nJ/pulse, and a VUV monochromator to cover the 6ω wavelength region.

A Ti:sapphire multipass amplifier (Dragon, KMLabs) generates 770 nm pulses (1.7 mJ/pulse, 25 fs) at 1 kHz. The output beam is split into two beams using a 70:30 splitter. The 70% portion of the beam is converted to 2ω (0.44 mJ/pulse) in a β-BaB_2O_4 crystal and gently focused using a dichroic concave mirror ($r = -2,000$ mm) into an Ne gas cell through a Brewster-angled CaF_2 window ($t = 1$ mm). The 30% portion of the fundamental beam (0.49 mJ) is focused into the same gas cell using another dichroic concave mirror ($r = -2,000$ mm). The temporal and spatial overlaps between the ω and 2ω pulses are adjusted by monitoring visible fluorescence from the Ne gas [10]. The ω and 2ω beams are aligned

 © 2014 Optical Society of America

collinearly with precision higher than 1 mrad in our setup. The gas cell has an aluminum pinhole plate 0.5 mm in thickness as the exit for laser pulses. Comparing with our previous study [9], we reduced the thickness of the plate by a factor of three, as laser-drilling of a thinner plate provides a three times larger pinhole diameter (ca. 0.3 mmϕ), which results in higher transmission of the laser pulses. The gas cell is connected to a multistage differential pumping system, in which the laser-drilled pinhole, a narrow channel (1.25 mm in diameter and 20 mm in length), and an aperture (3 mmϕ) restrict the gas conductance between the cell and an adjacent optics chamber maintained at $\sim 10^{-2}$ Torr [9]. The primary beams of ω and 2ω and the generated 3ω, 4ω, 5ω, and 6ω beams propagate collinearly and pass through the differential pumping system to enter the optics chamber.

Filamentation propagation is induced when an intense laser pulse self-focuses and ionizes a rare gas to create weak plasma. If we neglect optical influence of the plasma, the phase matching angle for noncollinear FWM of $2\omega + 2\omega - \omega \rightarrow 3\omega$ is predicted to be 1 mrad using the Sellmeier equation for neutral neon gas [11]. As can be seen in Fig. 1, similar calculations predict the phase matching angles for cascaded processes to generate 6ω to be from 1 to 4 mrad. We align the input laser beams collinearly with the precision higher than 1 mrad, so that the noncollinear phase matching is not operative in our experiment.

Figure 2 shows a setup for measurements of the pulse energy and the spectrum of 6ω. In pump–probe experiments, we separate the central and peripheral parts of the output beam using a flat UV-enhanced aluminum mirror with a 3 or 4 mm diameter hole [9]. However, in the measurement of the 6ω pulse energy, we reflected the entire output beam using five dichroic mirrors for 6ω (the specified reflectivity $R > 85\%$ for unpolarized light from 130 to 138 nm, Layertec) and sent the purified 6ω beam to a detector chamber housing a calibrated Si photodiode (SXUV, IRD) under vacuum. This optical layout effectively blocks the stray light from the optics chamber; however, a residual ω pulse propagating coaxially with 6ω creates a background signal at the detector. We evaluate this background signal by introducing air ($\sim$30 Torr) into the optical path to eliminate 6ω. The true 6ω pulse energy is determined by subtracting the pulse energy of ω from the energy measured under vacuum. The 6ω pulse is not observed when the input ω beam

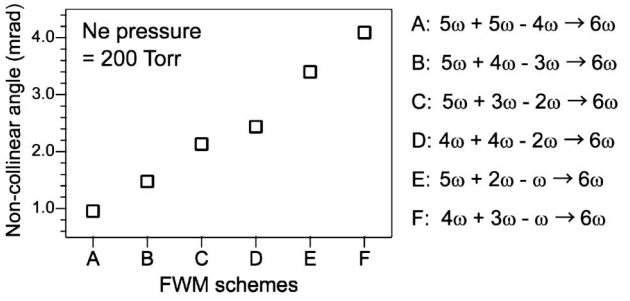

Fig. 1. Noncollinear angles expected for cascaded FWM processes to generate 6ω in neutral neon gas. The calculations were performed using Sellmeier equation given in [11] and the neon gas pressure of 200 Torr.

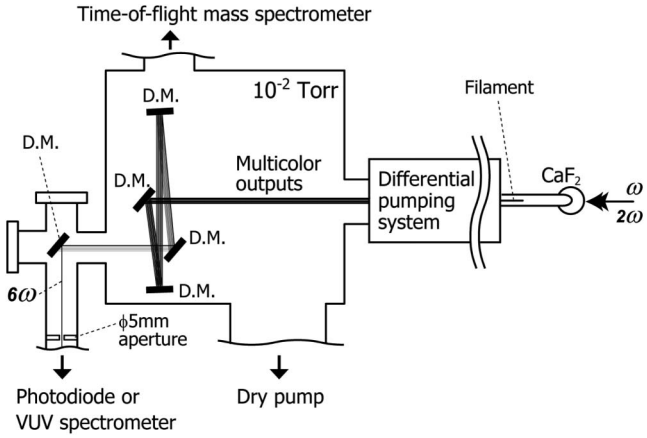

Fig. 2. Schematic diagram of our setup for measurements of the pulse energy and the spectrum of 6ω. D.M. denotes dichroic mirror.

is blocked, indicating that the direct third harmonics generation, $2\omega + 2\omega + 2\omega \rightarrow 6\omega$, is negligible.

Figure 3 shows the 6ω pulse energy as a function of Ne gas pressure in the cell. For comparison, the pressure dependence of the 3ω, 4ω, and 5ω pulse energies are also shown in arbitrary units. The 6ω pulse energy rapidly increases with the Ne gas pressure and exhibits its maximum (6 nJ/pulse) at around 200 Torr. Assuming 85% reflectivity of the mirror specified by the manufacturer, the 6ω pulse energy in the cell is estimated to be more than 10 nJ, corresponding to a conversion efficiency of ca. 2×10^{-5} with respect to the 2ω input pulse energy. The spatial profile of the 6ω pulse examined using a Ce:YAG phosphor plate was round below the gas pressures of ca. 200 Torr.

The 6ω pulse energy declines for Ne gas pressures higher than 200 Torr, even though the 3ω and 4ω pulse energies further increase. Qualitatively, the conversion efficiency increases with gas pressure, while it diminishes due to phase mismatch (Δk) at higher pressures when plasma created in filamentation propagation is neglected. Plasma dispersion will reduce phase mismatch, keeping conversion efficiency higher for low-order har-

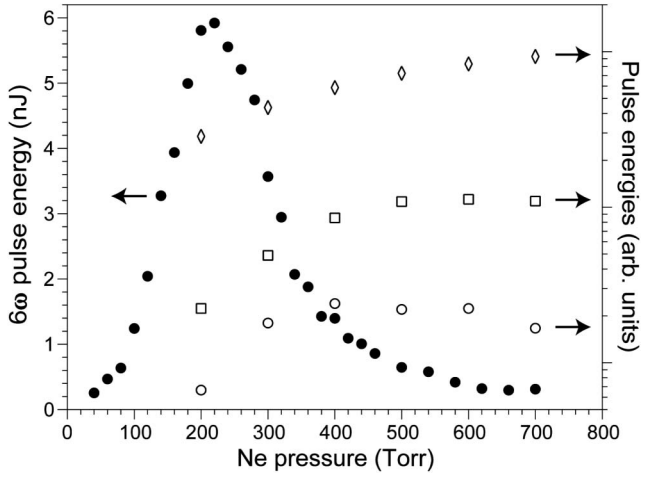

Fig. 3. Pressure dependence of the measured pulse energies for 6ω (solid circles). Pressure dependencies of the pulse energies for 3ω (diamonds), 4ω (squares), and 5ω (open circles) reported in [9] are also shown for reference.

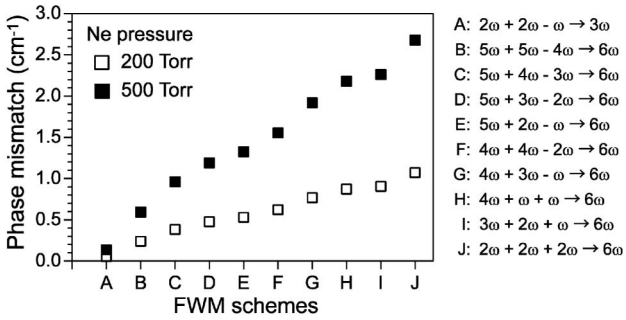

Fig. 4. Phase mismatch (cm^{-1}) expected for collinear FWM to generate 6ω in neutral neon gas. The calculations were performed using the Sellmeier equation given in [11] and the neon gas pressure of 200 (open squares) and 500 (solid squares) Torr. For comparison, the phase mismatch for $2\omega + 2\omega - \omega \rightarrow 3\omega$ is also shown.

monics with smaller dispersion. The drop of 6ω conversion efficiency at higher pressures is ascribed to the phase mismatch, which is too large to be compensated by the plasma. The phase mismatch in collinear FWM in neutral Ne gas can be calculated using the Sellmeier equation [11] as shown in Fig. 4. As seen here, Δk for $5\omega + 2\omega - \omega \rightarrow 6\omega$ is 10 times larger than that for $2\omega + 2\omega - \omega \rightarrow 3\omega$. Beutler *et al.* [6] observed that the intensity of 5ω generated by collinear FWM in argon ($3\omega + 3\omega - \omega \rightarrow 5\omega$) exhibits the maximum at 21 Torr and decreases at higher pressures. Similarly, Zuo *et al.* [8] observed that the pulse intensity of 5ω generated by cascaded FWM in argon ($4\omega + 3\omega - 2\omega \rightarrow 5\omega$) exhibits the maximum at 70 Torr and gradually declines at higher pressures. The appearance of these peaks in pressure dependencies of 5ω intensities is ascribed to dispersion much larger in argon than in neon. Thus, the pressure dependence of 6ω presented in this study is consistent with those of 5ω generated in Ar. More rigorous discussion on cascaded FWM processes and their pressure dependences requires complex three-dimensional model calculations taking into account the influence of plasma [10].

The spectrum of the 6ω pulse measured using a VUV monochromator (VM-502, Acton Research) is shown in Fig. 5. The spectrometer has been calibrated using a deuterium lamp. The resolution is estimated as 0.2 nm from

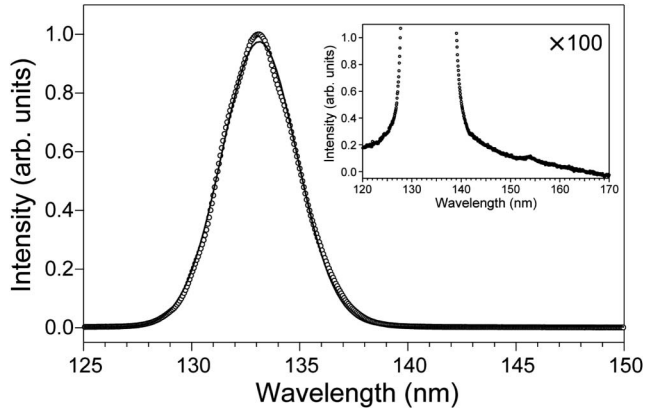

Fig. 5. Spectrum of the sixth harmonic (6ω) at the Ne gas pressure of 200 Torr is shown with circles. The solid line shows a Gaussian with a FWHM of 4.1 nm. An enlarged view of the spectrum from 120 to 170 nm region is also shown in the inset.

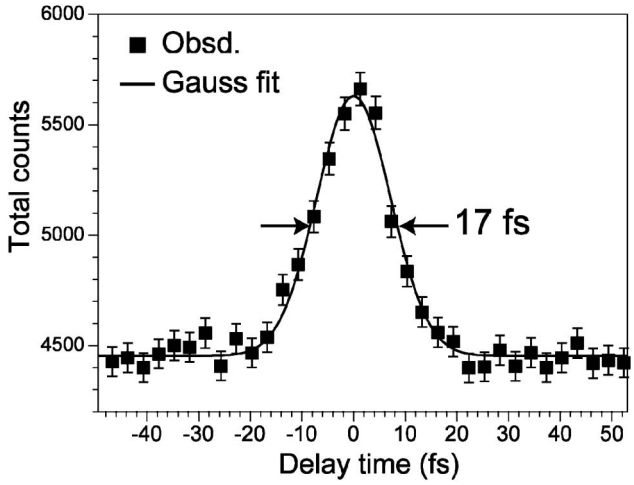

Fig. 6. Typical cross-correlation trace between 4ω and 6ω measured by nonresonant $(1 + 1')$ two-photon ionization of Kr atoms (squares). The solid line shows a Gaussian with a FWHM of 17 fs.

a full width at half-maximum (FWHM) of the Lyman-α line (121.5 nm). The 6ω spectrum exhibits a nearly Gaussian profile with a center wavelength at 133 nm. The 5ω component centered at 159 nm is absent, indicating that it is completely attenuated by the dichroic mirrors for 6ω. The observed spectrum shown in Fig. 5 supports a transform-limited pulse width of 6 fs.

Figure 6 shows the cross-correlation trace between the 4ω and the 6ω pulses measured using nonresonant $(1 + 1')$ two-photon ionization of krypton; the background (time-independent) signals are due to one-color two-photon ionization of 6ω pulses. Contribution of one-color three-photon ionization of krypton with 4ω pulses was negligible. As mentioned earlier, a flat UV-enhanced aluminum mirror with a 3 mm diameter hole is employed for the pump–probe measurements to separate the central and the peripheral parts of the output beams. The central part transmitted through the hole is reflected using five 6ω mirrors and focused by a concave 6ω mirror ($r = -1,000$ mm) onto an atomic beam of Kr. The peripheral part is reflected using four 4ω mirrors and focused by a concave aluminum mirror ($r = -1,000$ mm) with a UV-enhanced coating onto the Kr beam in overlap with 6ω. No dispersion compensation is made for 4ω nor 6ω. The Kr^+ photoion signal is measured using a microchannel plate detector and a single photon counter (SR400, Stanford Research Systems). The observed trace is fitted by a single Gaussian with a FWHM of 17 fs as shown in a solid line in Fig. 6. The FWHM of the cross-correlation is twice larger than 9.2 fs expected from the bandwidths of the 6ω and 4ω pulses. The pulse durations of the harmonics may be shortened by spectral phase transfer technique [12,13].

In conclusion, we have demonstrated sub-17 fs 6ω pulse generation with a sufficient pulse energy for pump–probe photoelectron spectroscopy. Our filamentation FWM light source can generate simultaneously 3ω, 4ω, 5ω, and 6ω at 1 kHz, enabling a variety of pump + probe schemes such as $3\omega + 4\omega$, $3\omega + 5\omega$, and $3\omega + 6\omega$, etc. Different wavelengths are easily selected using dichroic mirrors. Recently, Shi *et al.* [14] employed

2ω and 3ω of a high-power Ti:sapphire multipass amplifier (~50 mJ/pulse at 10 Hz) and generated 4ω, 6ω, 7ω (114 nm), 8ω (100 nm), and 9ω (89 nm) using FWM in Ar. Generation of higher harmonics than the sixth order would also be possible with a 1 kHz system.

References

1. F. Seifert, J. Ringling, F. Noack, V. Petrov, and O. Kittelmann, Opt. Lett. **19**, 1538 (1994).
2. V. Petrov, F. Rotermund, and F. Noack, Electron. Lett. **34**, 1748 (1998).
3. V. Petrov, F. Noack, D. Shen, F. Pan, G. Shen, X. Wang, R. Komatsu, and V. Alex, Opt. Lett. **29**, 373 (2004).
4. K. Kosma, S. A. Trushin, W. E. Schmid, and W. Fuß, Opt. Lett. **33**, 723 (2008).
5. F. Théberge, N. Aközbek, W. Liu, A. Becker, and S. L. Chin, Phys. Rev. Lett. **97**, 023904 (2006).
6. M. Beutler, M. Ghotbi, F. Noack, and I. V. Hertel, Opt. Lett. **35**, 1491 (2010).
7. M. Ghotbi, M. Beutler, and F. Noack, Opt. Lett. **35**, 3492 (2010).
8. P. Zuo, T. Fuji, T. Horio, S. Adachi, and T. Suzuki, Appl. Phys. B **108**, 815 (2012).
9. T. Horio, R. Spesyvtsev, and T. Suzuki, Opt. Express **21**, 22423 (2013).
10. T. Fuji, T. Suzuki, E. E. Serebryannikov, and A. Zheltikov, Phys. Rev. A **80**, 063822 (2009).
11. A. Börzsönyi, Z. Heiner, M. P. Kalashnikov, A. P. Kovács, and K. Osvay, Appl. Opt. **47**, 4856 (2008).
12. P. Zuo, T. Fuji, and T. Suzuki, Opt. Express **18**, 16183 (2010).
13. M. Beutler, M. Ghotbi, and F. Noack, Opt. Lett. **36**, 3726 (2011).
14. L. Shi, W. Li, H. Zhou, D. Wang, L. Ding, and H. Zeng, Phys. Rev. A **88**, 053825 (2013).